

Structure and Properties of Isotactic Polypropylene Oriented by Rolling with Side Constraints

Z. Bartczak, J. Morawiec, A. Galeski

Centre of Molecular and Macromolecular Studies, Polish Academy of Sciences, Sienkiewicza 112, 90-363 Lodz, Poland

Received 25 April 2001; accepted 7 February 2002

ABSTRACT: The rolling of isotactic polypropylene (iPP) with a new method of rolling with side constraints (inside a channel) was studied. It was found that deformation processes by compression in a channel die and by rolling with side constraints proceed in very similar fashions (plane-strain conditions) and result in materials of similar orientations and mechanical properties. The difference between the two processes is that rolling causes the destruction of the lamellar structure at a higher strain than compression. Dynamic mechanical measurements showed that rolling to a high strain produces not only a well-developed orientation of the crystalline component but also high orientation and transverse ordering of the amorphous phase, leading to its transverse anisotropy. iPP deformed by rolling with side constraints has tensile properties similar to those of iPP deformed by other methods, such as conventional rolling or

plane-strain compression. The elastic modulus and ultimate strength measured along the rolling direction increase with an increasing deformation ratio. For samples deformed to a deformation ratio of 10.4, the ultimate strength reaches 340 MPa and can be further increased by postdeformation annealing. The oriented iPP also demonstrates extremely high impact toughness, especially in the direction of side constraints. Izod impact tests demonstrated that the material fracture on impact is very limited and that the impact strength exceeds 170 kJ/m². In contrast to the tensile properties, there is an optimum deformation ratio around 5, for which the impact strength is the highest. © 2002 Wiley Periodicals, Inc. *J Appl Polym Sci* 86: 1413–1425, 2002

Key words: isotactic; mechanical properties; orientation; poly(propylene) (PP)

INTRODUCTION

The mechanical properties of a polymeric material can be greatly improved by its orientation.¹ In most cases, the molecular orientation leads to an increase in the material toughness and strength. The orientation of the chains in a polymer sample can be produced either by orientation of the molten or dissolved polymer or by plastic deformation in a solid state. The permanent deformation of polymeric materials in a solid state can be achieved by numerous methods, such as uniaxial and biaxial drawing, uniaxial compression, channel-die compression, rolling, solid-state extrusion, die drawing, and combinations of drawing with rolling or hydrostatic compression (for an overview, see refs. 1–6). The most common method of deformation used in both laboratory and industrial practice is cold drawing. Orientation by drawing has, however, a serious disadvantage, in that it is frequently accompanied by significant cavitation of the deformed polymer. Therefore, other techniques of orientation have been developed.

Among other known methods of plastic deformation, rolling is one of the best ways to produce a high preferred orientation (see refs. 7–18 for examples). Like compression modes, cavitation is usually not observed with rolling because of a high compressive stress component. Rolling is an attractive method of plastic deformation from an industrial point of view because it can be designed as a continuous process. However, the force required to roll significantly a wide strip of a polymeric material sometimes rises unacceptably high, whereas for rolling narrow strips, there is an unwanted component of transverse deformation deteriorating the final texture and, therefore, properties of the oriented material. A side effect of transverse deformation can be the formation of fissures, cracks, and cavitation at the edges of the rolled material.¹² These phenomena limit the use of rolling to the production of only relatively thin products in the form of films or tapes.

To overcome the limitations of conventional rolling, a novel method of obtaining highly oriented polymeric materials was developed recently. This method of rolling with side constraints^{19,20} is a combination of channel-die compression^{21,22} and rolling. This process relies on the rolling of a material inside a channel formed on the circumference of one roll with another roll having a width matching the width of the channel in the first roll. The side walls of the channel on the roll

Correspondence to: Z. Bartczak (bartczak@bilbo.cbmm.lodz.pl).

constitute lateral constraints as in a channel die. The other roll plays a role similar to that of a plunger in channel-die compression. The system of rolls with a channel develops conditions close to those of plane-strain compression of the rolled material. The plane-strain-compression mode is known to produce a well-developed single-component texture (quasi-single-crystal) of compressed materials.²¹ The advantage of such constrained rolling is the possibility of large strain deformation of relatively thick and wide and infinitely long bars or profiles in a continuous manner. The resulting profiles may have quite large cross-section areas and good mechanical properties, which could make them attractive engineering materials.

Recently, we applied constrained rolling to the high-strain orientation of high-density polyethylene (HDPE).^{23,24} We demonstrated that constrained rolling is essentially plane-strain compression like compression in a channel die and produces a texture similar to that of an oriented polyethylene. The obtained oriented bars exhibited high tensile strength and superior impact properties.

This article reports studies of the development of the orientation of isotactic polypropylene (iPP) through rolling with side constraints and the properties of resultant bars of highly oriented iPP. Orientation produced by constrained rolling is compared to that obtained by plane-strain compression in a channel die.

EXPERIMENTAL

Materials and procedures

Two commercial polypropylene homopolymers were used in this study. The first (iPP-1; EPP Kaprolan, DSM, Geleen, The Netherlands) had a melt-flow index at 2.16 kG and 230°C of 0.4 g/10 min and a density of 0.91 g/cm³ and was delivered in the form of extruded sheets 12 mm thick, whereas the other (iPP-2; Malen-P B200, Orlen SA, Plock, Poland) had a melt-flow index at 2.16 kG and 230°C of 0.6 g/10 min and a density of 0.91 g/cm³. The slabs, 100 mm × 12 mm and 1 m long, designed for rolling experiments, were machined from sheets of iPP-1. From iPP-2, the slabs, with 52 mm × 12 mm cross sections, were prepared by extrusion with a single-screw extruder (diameter = 32 mm) equipped with a water-cooled slot die.

The idea of constrained rolling is described in a previous article.²³ The rolling apparatus consists of two pairs of rolls with an effective (working) diameter of 280 mm. The lower roll in each set has an outer diameter of 480 mm and a channel cut out on the circumference to a depth of 100 mm and a width of 12 mm. The coworking upper roll has a diameter of 280 mm and a width of 12 mm, matching the channel in the lower roll. Other details of the setup are described in ref. 23.

The rolling of the slabs was performed on the aforementioned rolling apparatus. The rolling speed was usually set to 200 mm/min, although some experiments were performed at the highest speed of 4000 mm/min (the speed was the same for both sets of rolls), and the temperature of the rolls was kept at 90, 110, or 120°C. The iPP slabs were preheated to the desired temperature before being rolled in an oven. Then, they were deformed by being rolled to various deformation ratios (DRs), defined as the ratios of the initial and final cross sections of the sample, from DR = 2 to DR = 10.4. For higher DRs, it was necessary to roll a slab in several subsequent passes of smaller DRs.

For reference, samples of the same materials were compressed in a channel die as described in a previous article²⁵ at temperatures and deformation rates comparable to those applied in the rolling experiments.

Wide- and small-angle X-ray scattering

The texture of the rolled and compressed samples was examined with an X-ray pole figure technique. A wide-angle X-ray diffractometer system consisted of a computer-controlled pole figure attachment associated with a wide-angle goniometer coupled to a sealed-tube source of filtered Cu K α radiation operating at 30 kV and 30 mA. The following diffraction reflections from crystals of the monoclinic modification of iPP were analyzed: (110), (040), (130), (060), and ($\bar{1}$ 13) (with corresponding 2 θ diffraction angles of 14.1, 16.9, 18.5, 25.5, and 42.5°). Details for the procedure of pole figure determination are given elsewhere.²⁵

Lamellar orientation was probed by two-dimensional small-angle X-ray scattering (2D SAXS). A 1.1-m-long Kiessig-type camera was equipped with a pin-hole collimator providing point focus and with an imaging plate as a recording medium (Eastman Kodak, Rochester, NY). The camera was coupled to an X-ray generator (a sealed-tube, fine-point Cu K α filtered source operating at 50 kV and 35 mA from Philips, Eindhoven, The Netherlands). Exposed imaging plates were read out with a PhosphorImager SI scanner (Molecular Dynamics, Sunnyvale, CA).

Differential scanning calorimetry (DSC)

The melting behavior of the deformed samples was characterized with a TA 2100 differential scanning calorimeter (Thermal Analysis, New Castle, DE). The 5–8-mg specimens were cut from oriented samples in the plane perpendicular to the flow direction (FD). As a reference, a sample of unoriented iPP with a similar thermal history was also investigated. The DSC scans were made at a heating rate of 10°C/min.

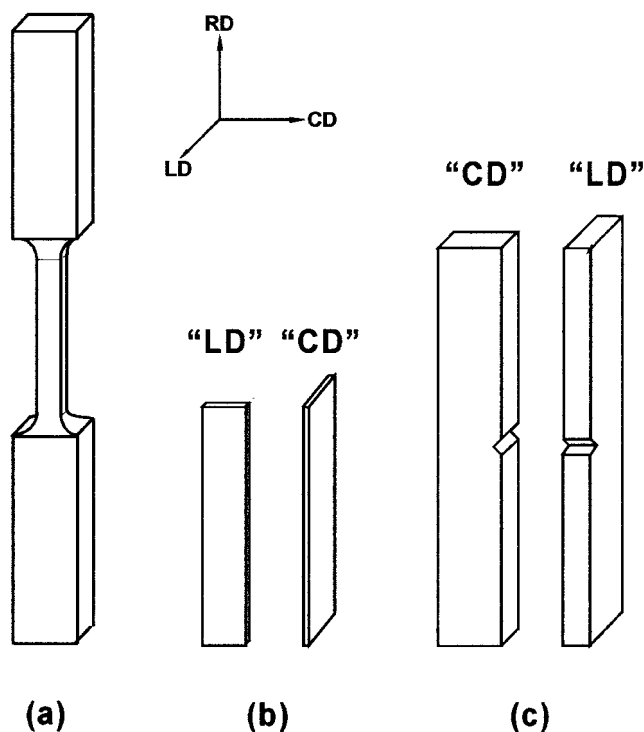


Figure 1 Geometry of the specimens used throughout this study: (a) a tensile specimen to be stretched in the RD, (b) specimens for dynamic mechanical studies to be bent in the LD and CD, and (c) notched Izod impact specimens to be loaded in the LD and CD. The reference axes of the rolled bar are RD, LD, and CD.

Mechanical measurements

Specimens for mechanical testing were prepared through the machining of bars of oriented polypropylene. Oar-shaped specimens designed for tensile testing had, in the narrow section, a length of 40 mm, a width of 5 mm, and a thickness of 2 mm. Wide parts on each side of the narrow section of the specimen were 50 mm × 10 mm × 6 mm so that a firm hold in the grips of the tensile machine was ensured. Figure 1(a) illustrates the orientation of a sample with respect to the reference directions of the oriented bar. These specimens were tested in a tensile mode at room temperature with an Instron model 1014 tensile machine (Instron Corp., Wycombe, UK). The crosshead speed of the machine was set to 2 mm/min, which corresponded to an initial deformation rate of 5%/min. An extensometer (25-mm gauge length) was used for measuring the sample elongation in the initial stage of deformation.

The dynamic mechanical properties of the deformed samples were measured with an Mk III dynamic mechanical thermal analyzer (Rheometric Scientific Inc., Epsom, UK) in a double-cantilever bending mode. The specimens, in the form of 50-mm-long, 8-mm-wide, and 1-mm-thick plates, were machined from deformed bars parallel to the rolling direction (RD) and

either the loading direction (LD) or constraint direction (CD), as shown in Figure 1(b). The first specimen was designed to bend along the LD, whereas the latter was designed to bend along the CD. The gauge length was 5 mm. The storage modulus (E') and loss factor ($\tan \delta$) were measured at a constant frequency of 1 Hz as functions of the temperature, which varied from -100 to 150°C at a heating rate of $2^\circ\text{C}/\text{min}$.

The impact properties of oriented bars were probed by notched Izod impact testing according to ISO Standard 180/1A. The 80 mm × mm 10 × 4 mm specimens were machined from oriented bars and notched with a type A notch (radius of notch base = 0.25 mm). Two sets of specimens of different orientations with respect to the reference directions of the bar were prepared for the determination of the impact strength of the material along the LD and CD, respectively. The geometry of the specimens is illustrated in Figure 1(c). The samples were tested at room temperature with an instrumented impact tester equipped with a hammer able to deliver 5.5 J of energy (Resil 5,5, CEAST S.p.A., Pianezza TO, Italy).

RESULTS AND DISCUSSION

Mechanical response to rolling

The rolling of iPP-1 and iPP-2 samples in this study was usually performed with the linear roll speed set at 200 mm/min at 90, 110, or 120°C . A few experiments were made with a high roll speed of 4 m/min, but then rolling was possible only to DRs lower than 5. For higher DRs, the friction forces between the rolled materials and the rolls were too low to drive the process, and the rolled bar decelerated and eventually stopped between rolls. Rolling to high DRs was not possible in a single step even at the low roll speed of 200 mm/min because of the very high forces generated during rolling that opposed the friction forces driving the process. Therefore, rolling in a few steps of lower DRs was necessary for the desired deformation to be reached. The friction forces in the apparatus employed in this study were considerably higher than those in conventional rolling¹² because of a special finish on the rolling surface of the rolls and an additional friction component between the rolled slab and side walls of the channel cut in the lower roll. Nevertheless, friction was too low for a high strain to be reached in a single step, especially at higher DRs, at which strain hardening of the material set in.

Neither necking nor cavitation phenomena were observed with rolling. Deformation was homogeneous in the entire strain range studied, like for that observed with compression in a channel die. Samples with a DR around 4 became translucent, in contrast to the opaque bars of virgin iPP. The samples with higher DRs became even more transparent; printed

letters were clearly visible through a rolled iPP-2 sample 9.5 mm thick (DR = 5.4). The force exerted on the rolls increased greatly with an increase in DR because of the strain hardening effect and despite a continuous reduction in the cross section of the rolled material. Measurements of the force generated on the upper roll at several DRs suggested that the stress-strain curve for rolling was quite similar to that observed in channel-die-compression experiments.²⁵ No fracture of the samples was observed even on heavy rolling up to a DR around 6. However, rolling to higher strains, above DR = 6, sometimes caused a limited fracture of the material along the RD, which led to partial delamination of the rolled bar in planes close to the rolled surface (i.e., that surface in contact with the roll). A tendency to fracture at large strains was stronger at low temperatures of the deformation process. Above DR = 7, occasionally some corrugations and warping of the rolled surfaces were also observed. The aforementioned fracture phenomena were caused by the superpositioning of two effects: (1) the slowing down of the rolled sample in comparison with the rolls due to high rolling forces opposing the friction between the rolls and the rolled bar and (2) the limited flow of the material into the narrow gap between the side wall of the lower roll and the upper roll. That material was forced to deform at a higher speed than the body of the bar, and this led to unwanted instabilities of deformation in the top layer of the rolled bar and, consequently, to some fracturing and warping within the skin layer of the bar. However, we did not observe any corrugations produced by differences in the strain across the width of the rolled bar like those described by Chaffey et al.¹² for conventional rolling. We believe that these undesirable effects can be eliminated from the process by a redesign of the rolls; rolling surfaces should be slightly rougher than in the actual setup for increased friction, whereas the gap between rolls should be minimized.

The rolled samples demonstrated substantial strain recovery after leaving the deformation zone between rolls. This strain recovery was short-term and ceased at a distance of approximately 20 cm or less beyond the last roll, depending on the temperature and deformation rate. Figure 2 presents the permanent strain plotted against the actual strain achieved in the deformation zone between rolls. The strain recovery increases with increasing DR up to a DR between rolls of less than 4 and then saturates and remains constant with a further strain increase. Such behavior indicates the presence of a quasielastic component within the structure of the rolled material, which apparently was not destroyed even by heavy rolling. This is discussed further in this section. Such recovery behavior was not observed previously in the compression of iPP in a channel die.²⁵ It was, however, observed in channel-die-compressed samples of ultrahigh molec-

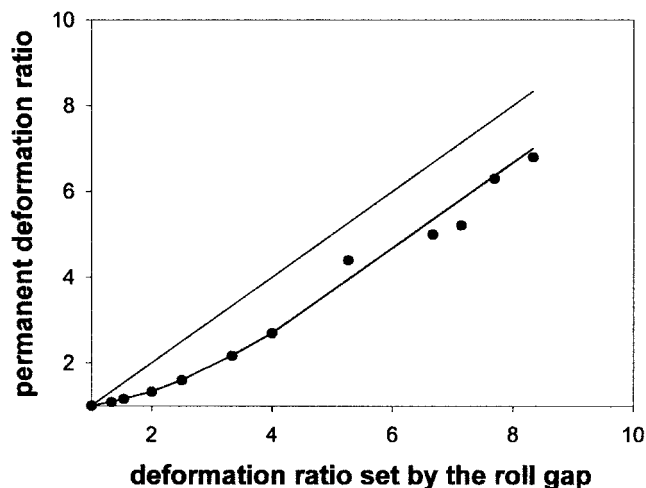


Figure 2 Dependence of the permanent strain and strain imposed on a sample during rolling, both expressed in terms of DR.

ular weight polyethylene.²⁶ We also observed very similar behavior in the rolling of high molecular weight polyethylene.²³ Note that both polypropylenes used in this study were high molecular mass grades. Moreover, a quasielastic recovery of comparable magnitude was observed in conventional rolling of iPP (weight-average molecular weight $\sim 6 \times 10^5$).¹²

The raw iPP slabs were imprinted with linear markers before rolling. The distance between markers was measured after each rolling pass. The macroscopic strain calculated from that distance between markers correlated well with that calculated from the reduction of the cross section of the rolled samples. The evolution of the shapes of the markers with increasing strain illustrates that rolling leads to nearly pure compression, with only a little macroscopic shear manifesting in a weak flow along the RD, especially in the range of low DRs. Such shear produces a slightly higher strain in the central part than near the rolled faces of the bar. However, with an increasing DR, the profile of the markers becomes curved and extends in the RD in the vicinity of both rolling faces. This supports another shear component, increasing with an increase in the overall strain. That shear and, therefore, the flow are strongest near the rolled faces. Consequently, at high DRs, the material develops higher local strain near the rolled faces of the bar than in its central part. These differences in the local strain supported by the unwanted side effects discussed previously are responsible for premature longitudinal fracture of the bar occurring near rolled surfaces.

Thermal properties and crystallinity

The melting behavior of the iPP-1 samples rolled to various DRs is illustrated in Figure 3. It shows that for

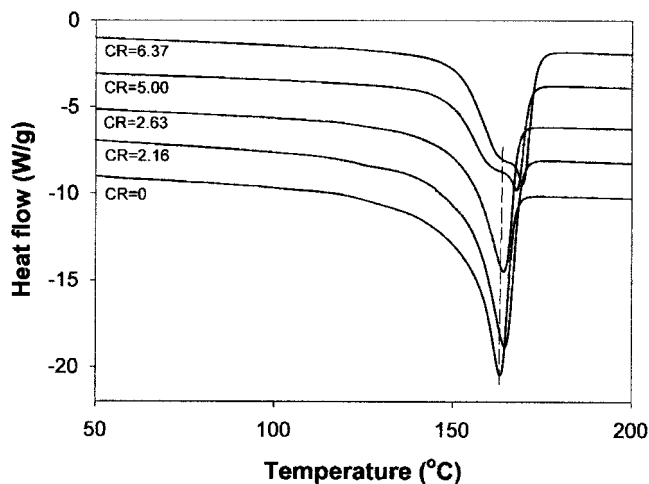


Figure 3 Melting curves of rolled iPP-1 samples deformed to the permanent DR indicated on each curve, as determined by DSC in a heating scan at a heating rate of $10^{\circ}\text{C}/\text{min}$.

low deformation, the melting peak is shifted slightly toward higher temperatures in comparison with undeformed iPP. However, at high deformation, above $\text{DR} = 5$, the temperature of the peak rises further, and an additional melting peak develops at a higher temperature. At the same time, the degree of crystallinity determined from the heat of fusion decreases continually with an increasing DR. At $\text{DR} = 6.37$, it is approximately 2% lower than in raw, undeformed iPP. An increase in the temperature of melting and a lowering of the crystallinity with increasing deformation demonstrates that a fraction of small crystallites is destroyed during the rolling process. The nature of the double melting peak observed at high deformation is not entirely clear. An artifact, resulting from the change in the thermal contact between the sample and DSC pan during the heating scan due to shrinkage of the highly oriented sample, cannot be excluded. However, Taraiya et al.,¹⁷ on the basis of detailed DSC studies supported by X-ray data of die-drawn polypropylene, suggested that heavy deformation leads to the formation of a new population of small crystallites in a different or disordered crystal form, the chain ends of which are constrained or which are in an extended chain form. That fraction of the crystalline phase may contribute to the second melting peak observed in samples deformed to a high strain. Because deformation by die drawing and rolling lead to comparable structures, it is feasible that here also such crystallites produced by high-strain deformation give rise to the additional melting peak.

Orientation of the crystallites

The evolution of the orientation of the crystallites in rolled samples of iPP was studied with an X-ray diffraction pole figure technique. Figure 4 presents pole

figures of the basic crystallographic planes of monoclinic polypropylene crystals (α form) determined for samples of iPP-1 rolled at 120°C and a speed of $200\text{ mm}/\text{min}$ to various DRs up to $\text{DR} = 6.4$. The pole figures of (110), (040), (130), and (060) crystallographic planes illustrate the orientation of the a and b crystallographic axes, whereas the pole figure of the $(\bar{1}13)$ plane is the best possible measure of the orientation of the chain axis because the monoclinic structure does not give any reflections of the (00 l) type, whereas the normal to the $(\bar{1}13)$ plane is only 5.8° away from the direction of the macromolecular chain axis, which is equivalent to the crystallographic c axis. The pole figures obtained for the iPP-1 samples rolled at 90°C and the samples of iPP-2 deformed under comparable conditions are very similar to those shown in Figure 4 and, therefore, are not presented here. Instead, Figure 5 shows a set of pole figures obtained for a sample of iPP-2 deformed to $\text{DR} = 6.4$ by channel-die compression at 110°C . A comparison of this set with the pole figures of the rolled sample with $\text{DR} = 6.37$ demonstrates that the crystalline textures of the rolled and compressed samples are nearly identical. A similar texture was reported also for iPP highly oriented by conventional rolling¹⁴⁻¹⁶ and die drawing.¹² Moreover, a comparison of the pole figures of rolled samples with lower deformation, shown in Figure 4, with the previously reported evolution of the texture of iPP compressed in a channel die²⁵ shows nearly identical evolution paths of the texture with increasing strain. This proves that the two deformation processes are very similar. We have found recently²³ that for linear polyethylene there is a close resemblance between the resulting structures of samples deformed through rolling with side constraints and channel-die compression. Both methods produce basically the same mode of deformation, a plane-strain compression.²³ Also here, for iPP the results of macroscopic observations of the deformation process and the resulting crystalline texture demonstrate that rolling results in plane-strain deformation similarly to compression in a channel die.

The final texture of the rolled bars of iPP at a DR above 6 is multicomponent. All identified components have a common sharp orientation of chain axis [001] along the RD. Two main components dominating the texture of a sample with $\text{DR} = 6.37$ were identified as (010)[001] and (110)[001]. At initial stages of the plastic deformation, [up to $\text{DR} = 2.63$; cf. Fig. 4(a,b)], the (100)[001] component developed first, but it was progressively replaced by the other texture components with increasing deformation. The identified deformation mechanisms leading to the formation of the final texture were (010)[001], (100)[001], and (110)[001] crystallographic slip systems, the same as those active during plastic deformation by channel-die compression.²⁵

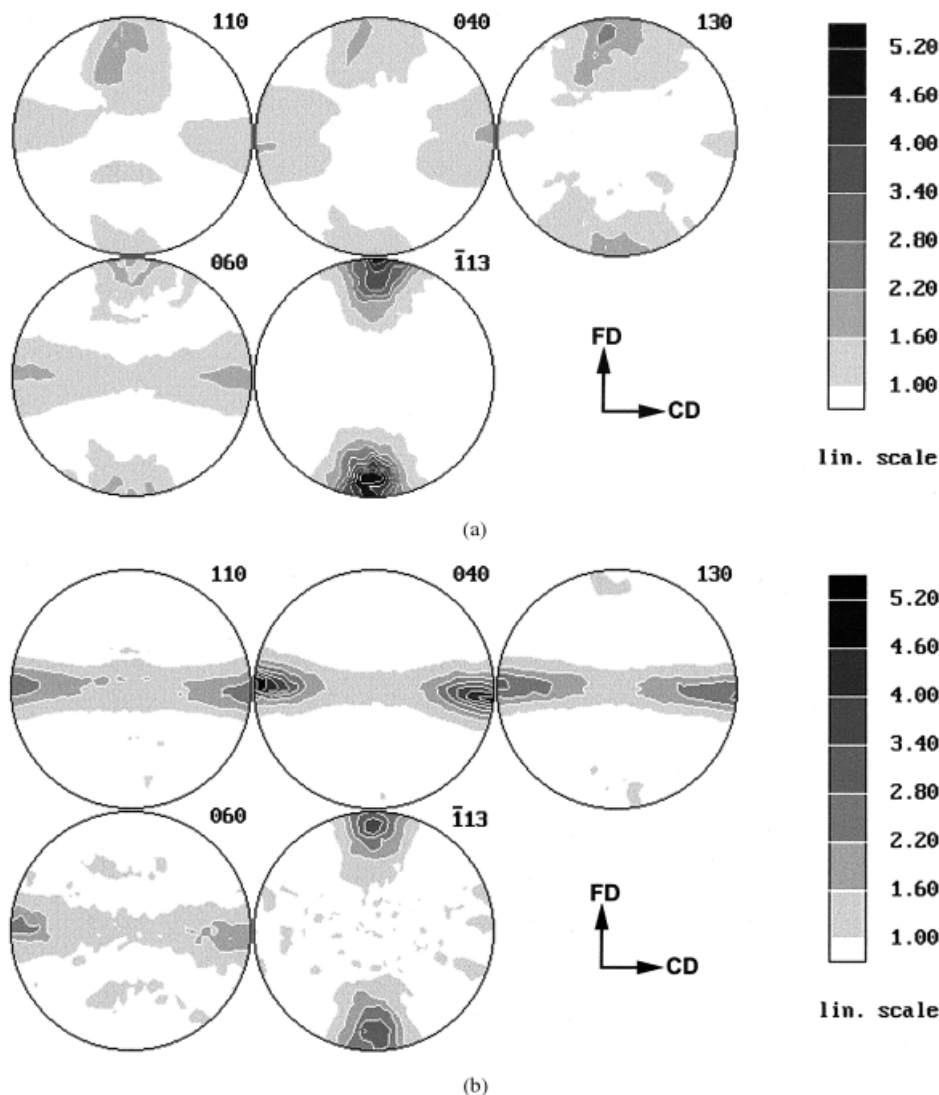


Figure 4 Pole figures of the (110), (040), (130), (060), and $\bar{1}13$ crystallographic planes of monoclinic polypropylene (α form) determined for samples of iPP-1 rolled at 120°C with a roll speed of 200 mm/min to the indicated permanent DR: (a) DR = 2.17, (b) DR = 2.63, (c) DR = 5.0, and (d) DR = 6.37. The figures are plotted in the stereographic projection. The RD is vertical, the CD is horizontal, and the LD is perpendicular to the projection plane in all figures.

Evolution of the lamellar structure

The lamellar structure of the deformed iPP samples was probed with 2D SAXS. Figure 6 displays 2D SAXS patterns obtained for samples of iPP-1 rolled to various DRs illuminated by an X-ray beam from either the CD or LD. The 2D pattern determined for the raw, undeformed slab demonstrates nearly isotropic orientation of lamellae on which a very weak orientation component is superimposed; a fraction of the lamellae are oriented preferentially with their normals perpendicular to the surface of the sheet from which the slab was cut (this direction becomes the CD direction with rolling). Additionally, a small equatorial streak can be observed in the pattern of the undeformed sample that indicates the presence of some microvoids in the initial material. The weak orientation and voids reflect

the manufacturing conditions of the plates by extrusion.

The LD-view pattern obtained for the sample deformed to the permanent DR of 2.17 is the superpositioning of an ellipse elongated in the RD and a somewhat stronger two-point pattern oriented in the RD. For higher DRs, the elliptical part of the pattern fades away, whereas the two-point component becomes stronger. At DR = 5 and DR = 6.37, only the two-point signature is present in the LD-view patterns. The CD-view patterns are more complex. At DR = 2.17, the pattern is the superpositioning of two long arcs oriented in the RD, a diffuse two-point pattern also oriented in the RD, and a four-point component, which is the strongest. For DR = 2.63, the arcs become shorter and merge with

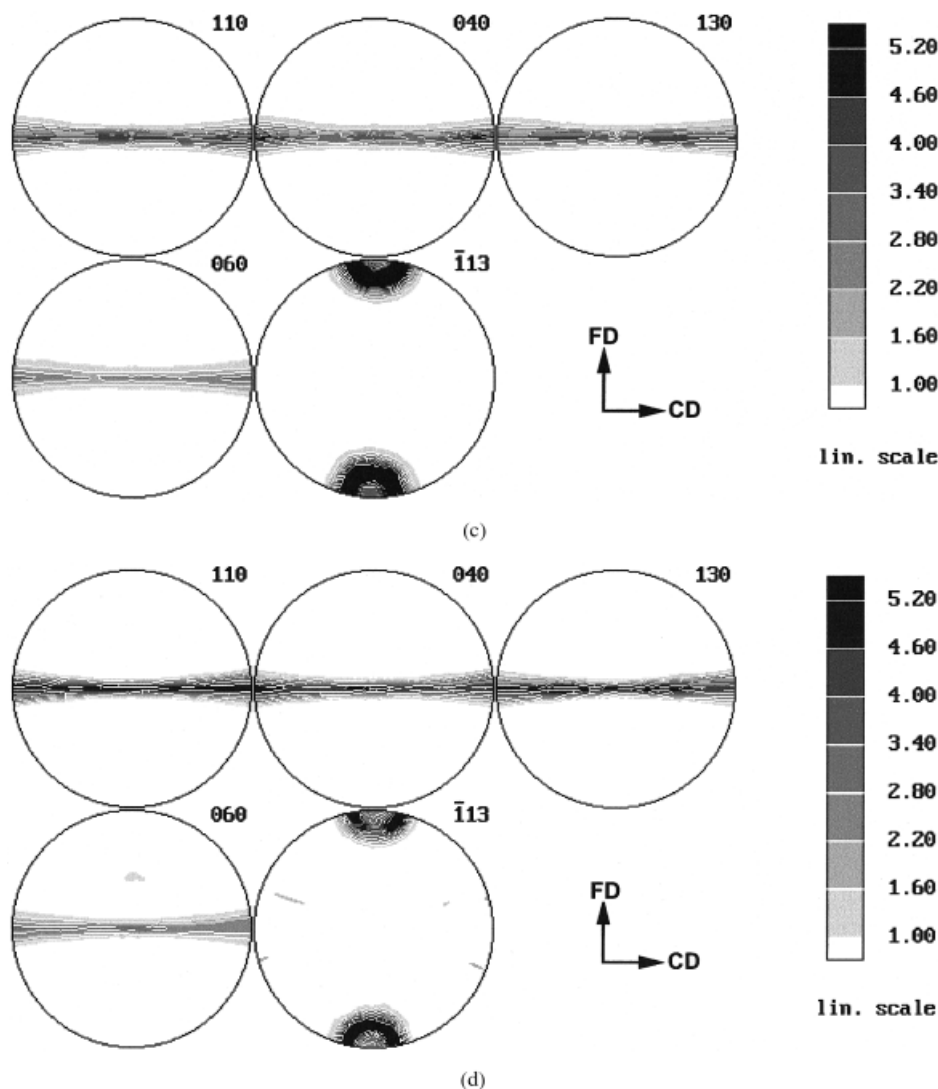


Figure 4 (Continued from the previous page)

the two-point component, elongating in the direction perpendicular to the RD (and parallel to the LD). The four-point part is hardly seen for this deformation. At higher deformations of DR = 5.0 and DR = 6.37, the CD-view pattern evolves further toward two lines oriented perpendicular to the RD. Along these lines, four weak maxima can be distinguished as the remnants of the four-point component. At the highest DR of 10.4, the features of both CD- and LD-view patterns remain the same as for DR = 6.37, yet the intensity of these patterns is a few times lower than at DR = 6.37. This suggests a progressive destruction of the lamellar structure.

In both CD- and LD-view patterns, the equatorial streak, which was observed for an unoriented sample, fades away with an increasing DR. This indicates the healing, during the rolling process, of the microvoids present in the raw material.

The discussed 2D SAXS patterns of rolled samples differ from those reported for channel-die-compressed samples.²⁵ In the channel-die-compression experiments, almost complete destruction of the lamellar structure was observed near a DR of 4, whereas in rolled samples that structure survived the deformation process up to a DR above 6, and even in a sample with DR = 10.4, its signature could still be recognized. In our recent studies of the rolling of HDPE, we also observed the presence of the lamellar structure in heavy rolled samples.²⁵ The shape of the CD patterns indicate that there was probably a cooperative kinking of the lamellae that allowed their reorientation without serious destruction during the rolling process. Lamellae were finally fragmented heavily, as demonstrated by the fading away of the scattering pattern for the sample of the highest DR, but this happened at a strain significantly higher than that for channel-die compression.

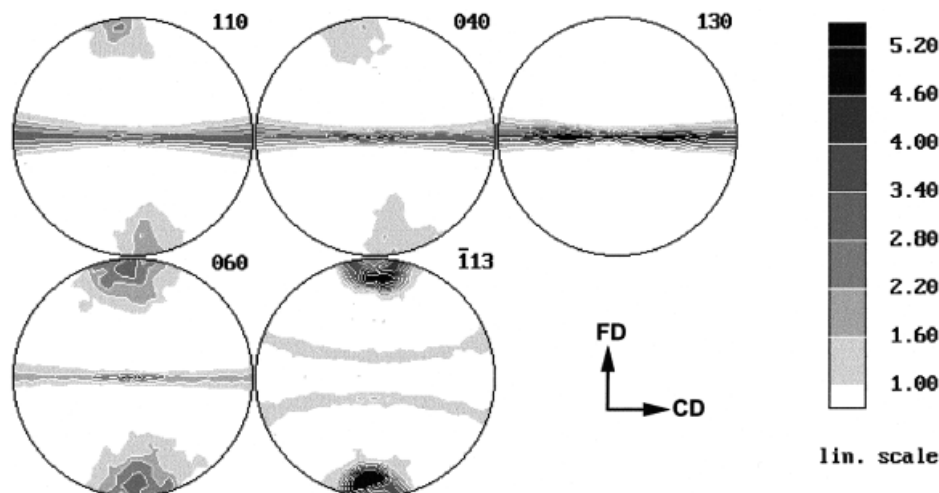


Figure 5 Pole figures (plotted in the stereographic projection) of the (110), (040), (130), (060), and $\bar{1}13$ crystallographic planes of monoclinic polypropylene (α form) determined for samples of iPP deformed at 110°C by channel-die compression to DR = 6.4. The FD is vertical, the CD is horizontal, and the LD is perpendicular to the projection plane.

Dynamic mechanical properties

The temperature dependencies of E' and $\tan \delta$ of an undeformed sample of iPP-2 and one rolled to a DR of 6.4 at 90°C are shown in Figure 7. For the deformed sample, two sets of curves are presented: one measured in the CD and the other in LD deformation geometry (cf. Fig. 1). All presented $\tan \delta$ curves reveal three mechanical relaxation processes typical for iPP: γ (around -50°C), β (near and above 0°C), and α (above 30°C).^{27,28}

The γ -relaxation process is assigned to the local relaxation mode, involving a few chain segments of the amorphous phase. Figure 7 shows that in the γ -relaxation region, the curves of $\tan \delta$ of the investigated samples exhibit a weak and broad maximum, the position of which is independent of the DR.

The maximum of the β relaxation is the most discernible maximum for the undeformed iPP. The β -relaxation process is usually attributed to the glass-rubber transition of the amorphous phase.²⁷ The position of this maximum at low frequencies can be assigned to the glass-transition temperature. As can be observed in Figure 7, the peak of the β relaxation decreases and shifts toward higher temperatures in oriented samples in comparison with that of undeformed materials. Similar observations were reported for iPP oriented by conventional rolling.²⁹ Such expected changes in the mechanical relaxation of the β process indicate clearly a substantial reduction in the mobility of the chains in the amorphous phase. As the overall crystallinity of the deformed samples is lowered only slightly in comparison with the undeformed iPP, the observed substantial damping of the β process with increasing strain should be interpreted in terms of a considerable change in the molecular packing of the amorphous phase resulting in reduced mobility. It

was demonstrated for uniaxially compressed iPP^{30–32} that the density of the amorphous phase increased markedly with increasing strain, which indicated that the average intermolecular distance was smaller than the respective distance in the unoriented amorphous component.

Another important finding is that the position of the maximum of the β relaxation in the oriented sample depends on the test geometry. When the specimen was loaded along the CD (CD geometry; cf. Fig. 1), this maximum was found at a temperature approximately 1°C higher than the maximum observed when the specimen was loaded along the LD (LD geometry). We must note that this shift is not an artifact because we observed this effect in many independent measurements. Moreover, we found similar behavior in the γ relaxation of rolled HDPE²⁴ and samples oriented by channel-die compression (both iPP and HDPE). This effect of the anisotropic response can be an indication of the transverse anisotropy (i.e., in the plane perpendicular to the direction of molecular orientation) of the highly oriented amorphous phase of rolled iPP. In samples of highly oriented HDPE, which also show similar mechanical anisotropy, a careful examination of X-ray scattering³³ disclosed that high-strain deformation in plane-strain compression leads to the ordering of the amorphous phase with the formation of pseudo-hexagonal packing, in which the chains axes are oriented along the FD and the (100) pseudoplane is oriented parallel to the LD. Such ordering causes an increase in the density of the non-crystalline component and should, of course, induce serious modifications of its properties, including the relaxation behavior. Moreover, the reorganization of the lamellar structure occurring at a high plastic strain results in stronger constraints imposed on the interla-

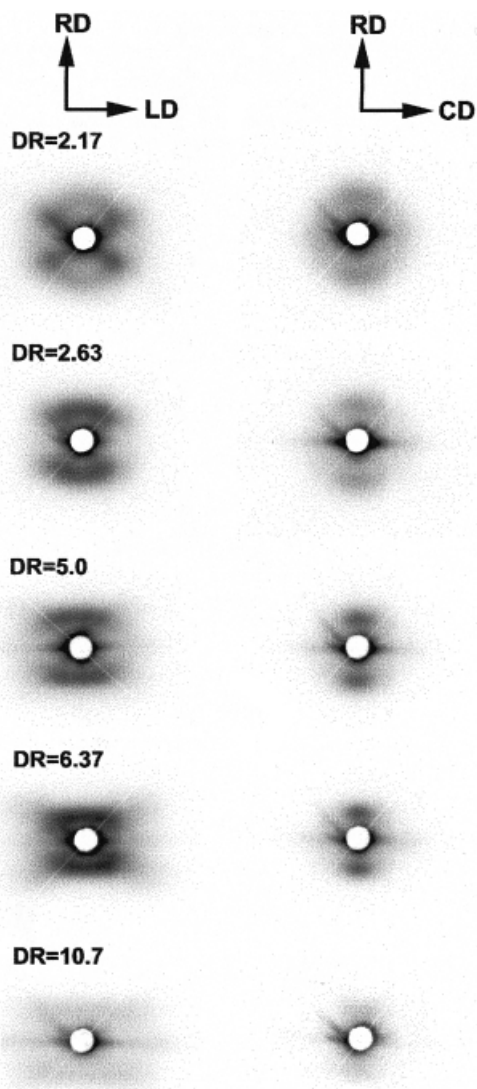


Figure 6 2D SAXS patterns obtained in LD and CD illumination views for samples of iPP-1 rolled at 120°C with a roll speed of 200 mm/min to the indicated DR.

mellar amorphous material, which is intimately connected to the orienting crystallites. That increase in the constraints will make amorphous layers stiffer than those in the undeformed sample and, consequently, will result in the modification of the mechanical response of the oriented sample. Taking all this into consideration, one can expect an anisotropy of the mechanical response of the oriented samples in their LD-CD plane.

The α -relaxation process manifests itself with an increase in $\tan \delta$ at a temperature greater than 30°C. As can be observed in Figure 7, $\tan \delta$ of the undeformed sample increases gradually with temperature in the temperature range of the α relaxation. The curves of $\tan \delta$ of the deformed sample also rise in this temperature range, yet with the slope much steeper than the slope of the curve of undeformed iPP. Addi-

tionally, a distinct maximum develops for the oriented sample. This maximum is related in part to the shrinkage of the rolled sample as the temperature approaches the temperature of rolling. Considering this, one can suppose that the α process in the deformed samples is strongly supported by the phenomena of the relaxation of the orientation in the noncrystalline component in interlamellar regions, probably because of the activation of shrinkage phenomena. A similar conclusion was drawn previously in a study of iPP deformed in a channel die.²⁵

Tensile properties

Figure 8 shows representative stress-strain curves of the specimens cut from bars of iPP oriented through rolling with side constraints (iPP-1, deformed at 120°C) to various DRs. All the specimens were tested in tension along the direction of the molecular orientation, which coincided with the RD. All tensile tests were performed at room temperature with a constant crosshead speed of 2 mm/min, which corresponded to an initial deformation rate of 5%/min. The numerical values of the mechanical parameters determined from the curves are reported in Table I. These data show a continuous increase in both the modulus and ultimate tensile strength with an increasing DR, which is a typical effect of orientation. The maximum strength at the level of 340 MPa is achieved for a

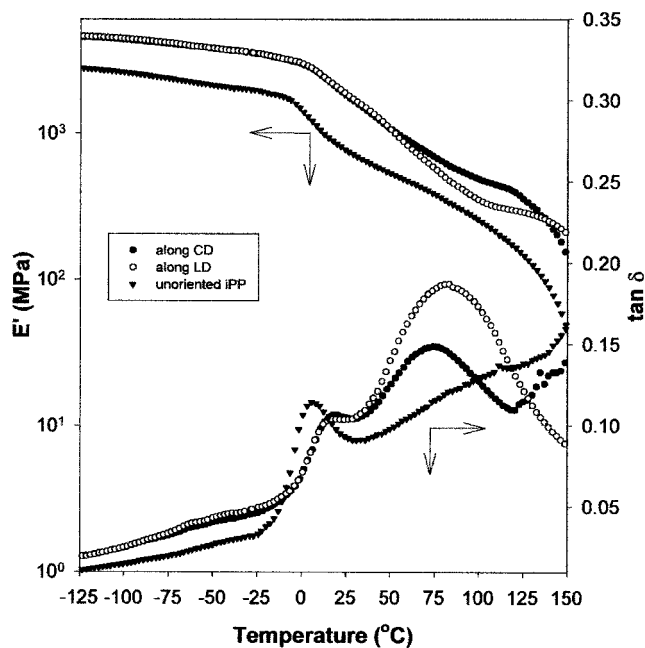


Figure 7 Dynamic mechanical thermal analysis curves determined in a double-cantilever bending mode at a frequency of 1 Hz and at a heating rate of 2°C for samples of iPP-2 undeformed and rolled to DR = 6.4: E' and $\tan \delta$. Two curves representing the rolled sample probed in the CD and LD are shown.

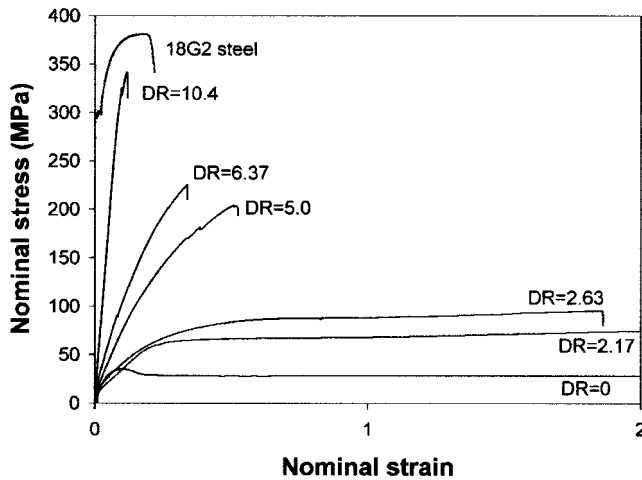


Figure 8 Exemplary nominal stress/nominal strain curves determined for the tensile deformation of rolled iPP-1 samples with various DRs indicated on each curve. Tensile tests were performed at room temperature, and the initial deformation rate was 50%/min. The curve for 18G2 concrete reinforcing steel is plotted for comparison.

sample with DR = 10.4. The obtained values are similar to those reported in the literature for iPP deformed by various special techniques to a comparable strain.³⁴ In Figure 8, the stress-strain curve for 18G2 concrete reinforcing steel is also plotted for comparison. The strength of rolled iPP (DR = 10.4) is comparable to that for steel, although its elastic modulus is 1 order of magnitude lower than that of the steel.

The rolled samples demonstrate a slightly lower Young's modulus and ultimate tensile strength but a higher elongation to break than the samples obtained by channel-die compression to a comparable strain. Annealing of the rolled sample at a temperature above the deformation temperature reduces the difference in strength in comparison with the channel-die-compressed material, yet the ultimate elongation remains higher than that in the channel-die sample. This is illustrated in Figure 9 for the sample of iPP-2 deformed by both rolling and channel-die compression to similar permanent DRs (6.4 and 6.5 for the rolled and compressed samples, respectively).

TABLE I
Tensile Data of the Rolled iPP

DR	Elastic modulus (MPa)	Tensile strength (MPa)	Ultimate elongation (%)
1	0.96	34	450
2.17	2.04	76	225
2.63	2.70	97	180
5.00	4.08	202	49
6.37	4.66	215	33
10.40	6.30	341	18

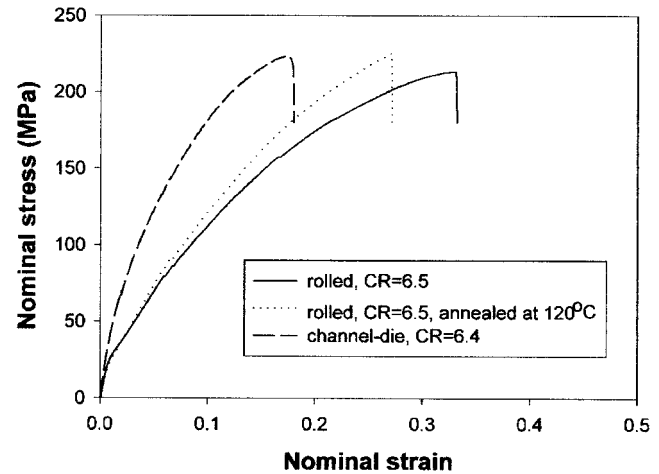


Figure 9 Tensile stress-strain curves for samples of iPP-2 deformed by channel-die compression (DR = 6.5) and rolling (DR = 6.4). The third curve is for a rolled sample (DR = 6.4) annealed after rolling at 120°C at a constant length.

Impact properties

Impact properties of the rolled bars were probed with an instrumented notched Izod test performed at room temperature. Specimens for testing were cut from rolled bars along the RD with the notched face perpendicular either to the LD or CD (cf. Fig. 1) for the determination of the toughness of the material along those two directions.

Figure 10 presents a photograph of the impact specimens of iPP-1 after Izod testing. The undeformed specimen and the specimen with DR = 2.17 tested along the LD broke completely. The Izod impact strength of the undeformed iPP was 4.6 kJ/m², whereas for the specimen with DR = 2.17 tested along the LD, it increased nearly twofold to 8.1 kJ/m². The other tested samples did not break, and only limited fracture and delamination could be observed. Figure 10 shows that in the specimens tested along the LD, the delamination initiated by the notch spread out along planes approximately perpendicular to the LD direction. The area of the fracture decreases with increasing DR up to DR = 5.0. For the sample with DR = 6.37, the area of the fracture planes is again larger than in the sample with DR = 5.0. In samples tested along the CD, a more complicated fracture geometry was observed. For low DRs, samples fractured near the notch mostly along planes perpendicular to the direction of impact (which was the CD). At DR = 5.0, short cracks developed along planes both perpendicular and parallel to the CD. In a sample with DR = 6.37, few cracks were formed in planes parallel to the CD and perpendicular to the LD. For each DR, the total surface of the cracks developed in the samples tested along the CD was smaller than that in the samples tested along the LD. This observation agrees with the force and energy data determined from the

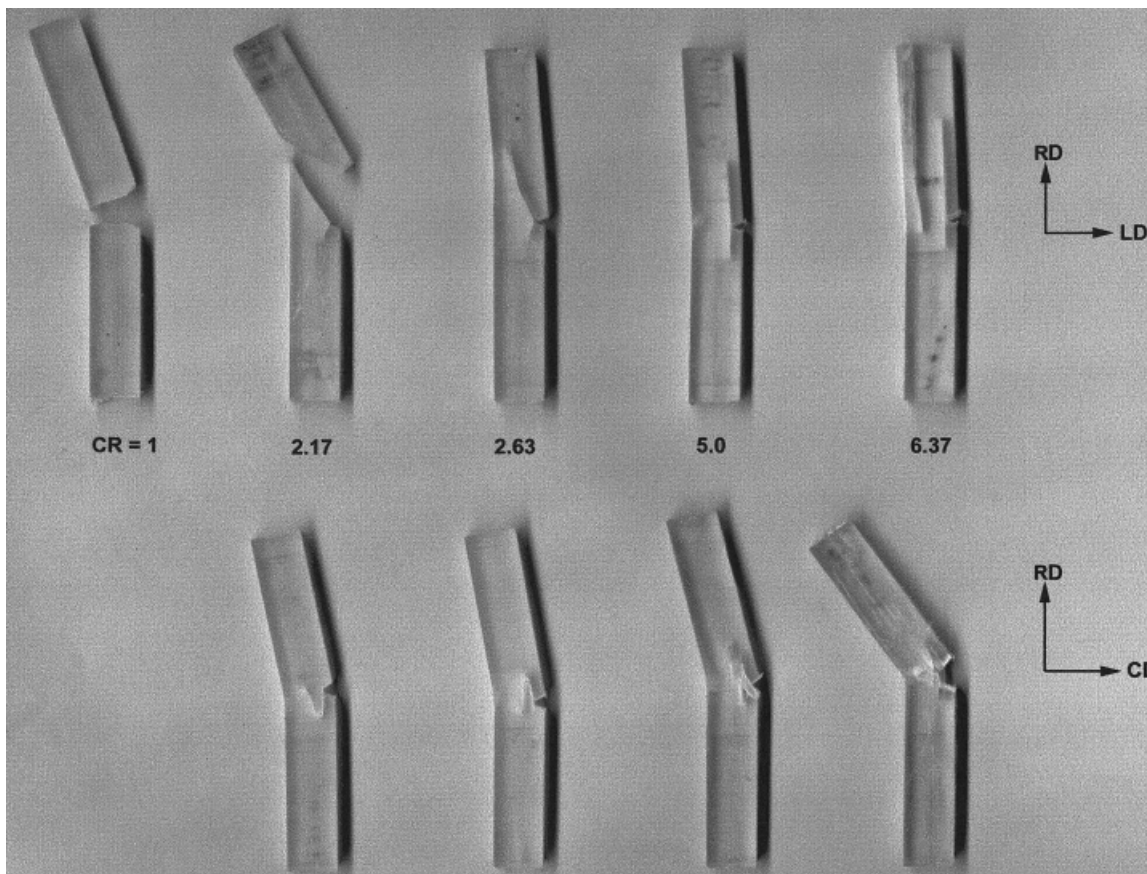


Figure 10 Photograph of Izod specimens after impact testing. The upper row shows specimens tested along the LD, and the lower row shows those tested along the CD. The DRs of the samples are indicated.

time-force curves acquired during impact. Figure 11 shows the peak force on the time-force curve, the portion of energy dissipated at this point, and the total energy dissipated during the impact test plotted against the DR. Data for both LD and CD test geometries are presented. The peak force and energy can be connected with the initiation and propagation of fracture, whereas the remaining energy was dissipated mostly for plastic deformation (bending) of the unbroken portion of the sample. The energy data demonstrate that more energy is consumed by the latter process than by cracking. The higher peak force and energy observed for samples tested along the CD confirm the observation that the preferred plane of the fracture (i.e., less energy consumed) is the plane perpendicular to the LD rather than the plane perpendicular to the CD. The peak force increases steadily with the increase in the DR. However, the dependencies of the peak and total energy dissipated on the DR indicate a maximum near a DR of 5. For this DR, the smallest area of the fracture was observed. The energy dissipated during the impact of the sample with DR = 5, tested in both LD and CD geometries, reached the capacity of the hammer used, 5.5 J. An impact strength greater than 170 kJ/m² would correspond to the dis-

sipation of such energy. This is almost a 40-fold increase in comparison with that of an unoriented sample of iPP. We previously observed a similar enormous increase in the impact strength of HDPE oriented through rolling with side constraints.²⁵ The optimum impact strength near DR = 5, at which ratio the toughness of the oriented material was the highest, was also found for HDPE. One should also note other literature reports describing an extremely high toughness achieved in oriented iPP products. For example, the BeXor process (Bethlehem Steel Corp., Bethlehem, PA)³⁵ can make biaxially oriented polypropylene sheets with a toughness more than 10 times higher than that of raw, unoriented materials.^{36,37} The BeXor sheets appear sufficiently tough to stop a 35-mm bullet.³⁶

CONCLUSIONS

Cavitation occurring during plastic deformation frequently reduces considerably the strength of oriented polymeric materials. Cavity-free deformation such as plane-strain compression in a channel die leads to oriented polymeric materials with a strength higher than that of a material oriented by deformation with no constraints imposed. In that deformation mode, the

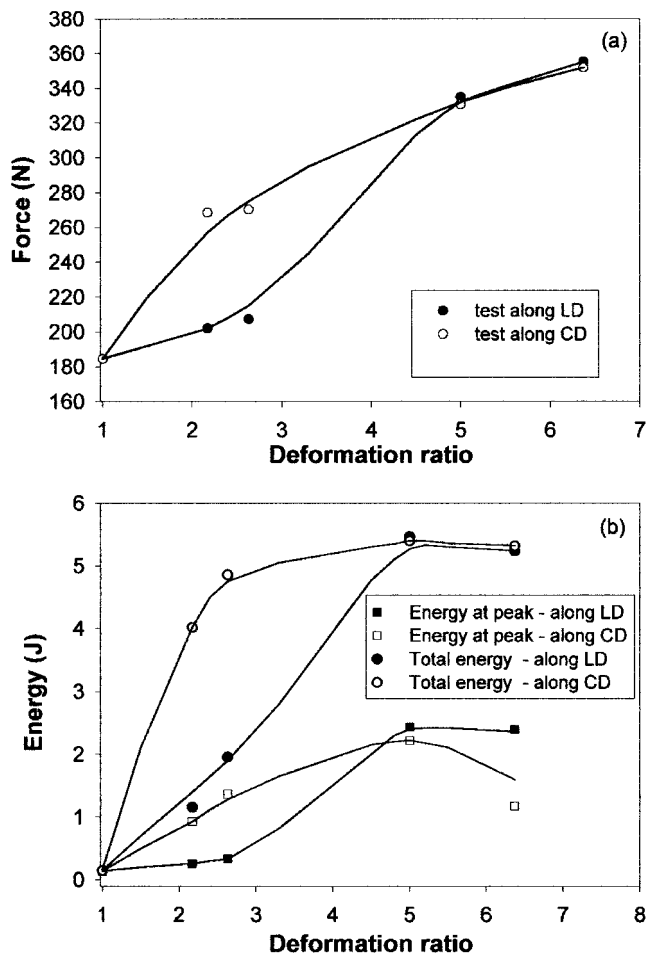


Figure 11 (a) Peak force and (b) peak energy and total energy dissipated, as determined from time-force curves obtained in Izod impact testing of samples of rolled iPP-1, plotted as functions of their DRs.

side constraints imposed on the material during its compression help to prevent unwanted cavitation and to produce materials with well-defined and sharp textures. The new method of rolling inside a channel, reported here, resembles to a large extent plane-strain compression in a channel die. We have shown that the deformation processes of iPP by compression in a channel die and by rolling with side constraints proceed in very similar fashions and result in materials of similar orientations and mechanical properties. Like channel-die compression, rolling produces nearly plane-strain deformation with only a minor flow component within the skin layer. The crystalline textures and lamellar orientations of iPP samples resulting from deformation by both methods are similar at corresponding strains. The only difference is that rolling causes the destruction of the lamellar structure at a higher strain than compression does.

iPP deformed by rolling with side constraints has tensile properties similar to those of iPP deformed by other methods, such as conventional rolling or plane-

strain compression. The elastic modulus and ultimate strength measured along the RD increase with an increasing DR. For samples deformed to DR = 10.4, the ultimate strength reaches 340 MPa and can be further increased by postdeformation annealing.

Along with very good tensile properties, the oriented bars of iPP demonstrate extremely high impact toughness, especially in the direction of the side constraints (CD). The Izod impact tests demonstrated that the fracture on impact is very limited and that the impact strength of the bars must exceed 170 kJ/m². It is concluded that the greater part of the energy is dissipated by the bending of unbroken parts of the sample. In contrast to the tensile properties, there is an optimum DR around 5, for which the impact strength is the highest. For higher orientation, more cracks develop during impact, and the energy absorbed for the bending of the sample is slightly lower.

Dynamic mechanical measurements showed that heavy rolling to a high strain (DR > 6–7) produces a well-developed orientation of the crystalline component and also high orientation and transverse ordering of the amorphous phase, which leads to the anisotropy of their properties in the LD-CD plane perpendicular to the RD.

Orientation through rolling with side constraints allows for the continuous production of oriented materials of unlimited length, similarly to conventional rolling, yet with relatively large cross sections (>1 cm²). Because of their large size and very good mechanical properties, the rolled bars or profiles produced from commodity polymers such as iPP may become very attractive engineering materials.

References

1. Ward, I. M.; Hadley, D. W. *Introduction to Mechanical Properties of Solid Polymers*; Wiley: New York, 1993.
2. *Solid Phase Processing of Polymers*; Ward, I. M.; Coates, P. D.; Dumoulin, M. M., Eds.; Hanser: Munich, 2000.
3. *Ultra-High Modulus Polymers*; Ciferri, A.; Ward, I. M., Eds.; Applied Science: London, 1979.
4. Bowden, P. B.; Young, R. J. *J Mater Sci* 1974, 9, 2034.
5. *Plastic Deformation of Amorphous and Semicrystalline Materials*; Escaig, B.; G'Sell, C., Eds.; Editions de Physique: Paris, 1982.
6. Lin, L.; Argon, A. S. *J Mater Sci* 1994, 29, 294.
7. Frank, F. C.; Keller, A.; O'Connor, A. *Philos Mag* 1958, 3, 64.
8. Yoda, O.; Kuriyama, I. *J Polym Sci Polym Phys Ed* 1977, 15, 773.
9. Tate, K. R.; Perrin, A. R.; Woodhams, R. T. *Polym Eng Sci* 1988, 28, 1264.
10. Burke, P.; Weatherly, G. C.; Woodhams, R. T. In *High Modulus Polymers: Approaches to Design and Development*; Zachariades, A. E.; Porter, R. S., Eds.; Marcel Dekker: New York, 1988; p 459.
11. Yang, J.; Chaffey, C. E.; Vancso, G. J. *Plast Rubber Process Appl* 1994, 21, 201.
12. Chaffey, C. E.; Taraiya, A. K.; Ward, I. M. *Polym Eng Sci* 1997, 37, 1774.
13. Kaito, A.; Nakayama, K.; Kanetsuna, H. *J Appl Polym Sci* 1985, 30, 1241.

14. Dhingra, V. J.; Spruiell, J. E.; Clark, E. S. *Polym Eng Sci* 1981, 21, 1063.
15. Hibi, S.; Niwa, T.; Wang, C.; Kyu, T.; Lin, J.-R. *Polym Eng Sci* 1995, 35, 902.
16. Hibi, S.; Niwa, T.; Mizukami, J.; Wang, C.; Kyu, T. *Polym Eng Sci* 1995, 35, 911.
17. Taraiya, A. K.; Unwin, A. P.; Ward, I. M. *J Polym Sci Part B: Polym Phys* 1988, 26, 817.
18. Krause, S. J.; Hosford, W. F. *J Polym Sci Part B: Polym Phys* 1989, 27, 1867.
19. Bartczak, Z.; Galeski, A.; Morawiec, J.; Przygoda, M. *Pol. Pat. PL-178058* (1995).
20. Morawiec, J.; Bartczak, Z.; Kazmierczak, T.; Galeski, A. *Mater Sci Eng A* 2001, 317, 21.
21. Song, H. H.; Argon, A. S.; Cohen, R. E. *Macromolecules* 1990, 23, 870.
22. Galeski, A.; Bartczak, Z.; Argon, A. S.; Cohen, R. E. *Macromolecules* 1992, 25, 5705.
23. Bartczak, Z. *J Appl Polym Sci* 2002.
24. Bartczak, Z.; Morawiec, J.; Galeski, A. *J Appl Polym Sci* 2002.
25. Pluta, M.; Bartczak, Z.; Galeski, A. *Polymer* 2000, 41, 2271.
26. Boontongkong, Y.; Cohen, R. E.; Spector, M.; Bellare, A. *Polymer* 1998, 39, 6391.
27. Boyd, R. H. *Polym Eng Sci* 1979, 19, 1010.
28. Jourdan, C.; Cavaillie, J. Y.; Perez, J. *J Polym Sci Part B: Polym Phys* 1989, 27, 2361.
29. Nakayama, K.; Kun, Q.; Hu, X. *Polym Polym Compos* 2001, 9, 151.
30. Osawa, S.; Porter, R. S. *Polymer* 1994, 35, 540.
31. Osawa, S.; Porter, R. S. *Polymer* 1994, 35, 545.
32. Osawa, S.; Porter, R. S. *Polymer* 1994, 35, 551.
33. Bartczak, Z.; Galeski, A.; Argon, A. S.; Cohen, R. E. *Polymer* 1996, 37, 2113.
34. Bigg, D. M. *Polym Eng Sci* 1976, 16, 725.
35. Austen, A. R.; Humphries, D. V. *U.S. Pat. 4,282,277* (1981).
36. Austen, A. R.; Humphries, D. V. *Soc Plast Eng Annu Tech Conf Tech Pap* 1982, 837.
37. Pan, S. J.; Tang, H. I.; Hiltner, A.; Baer, E. *Polym Eng Sci* 1987, 27, 869.